THE JOURNAL OF PHYSICAL CHEMISTRY C

ARTICLE

pubs.acs.org/JPCC

Optical Reorientation and Trapping of Nematic Liquid Crystals Leading to the Formation of Micrometer-Sized Domain

Anwar Usman,*,† Takayuki Uwada,*,† and Hiroshi Masuhara*,†,‡

†Department of Applied Chemistry and Institute of Molecular Science, National Chiao Tung University, Hsinchu 30010, Taiwan

‡Graduate School of Materials Science, Nara Institute of Science and Technology, 8916-5 Takayama, Ikoma 630-0192, Japan

ABSTRACT: We report on observation of optical reorientation of homogeneous nematic liquid crystals (LCs) thin slab of 4′-penthyl-4-cyanobiphenyl induced by a tightly focused near-infrared laser beam. We found that for laser beam with intensity higher than 56 MW/cm^2 the optical reorientation unusually transforms to a new metastable domain, which grows with laser irradiation time up to a dimension much larger than that of the focal spot. The optically reoriented LCs with refractive index mismatch compared to the surroundings can act as a micrometer-sized "ghost particle", leading to the generation of optical trapping and manipulation of the optically reoriented LCs. By using confocal Raman microspectroscopy, we show that the dichroic ratio in the confined focal volume changes upon the domain formation with an increase in the total Raman intensity, indicating that microscopic depolarization leading to deorientation or nematic → isotropic phase transition and possible microscopic densification takes place by the tightly focused laser beam.

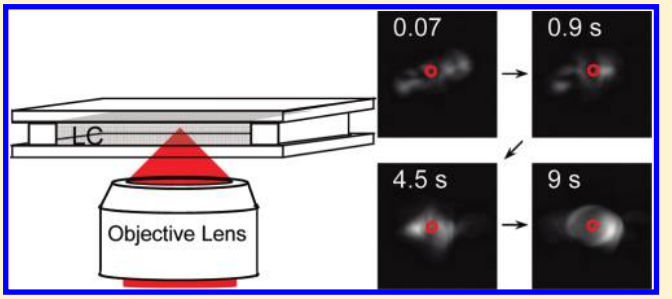

1. INTRODUCTION

The specific properties of liquid crystals (LCs) as a fluid with a long-range order of anisotropy, large birefringence, and excellent spatiotemporal cooperative motions are responsible for many optical processes in LCs. The most fascinating process is optical reorientations of nematic LC director in response to an applied optical field of a conventional illumination light. In this process, the optical field above optical Fréedericksz transition (OFT) threshold (usually in the order of kW/cm^2) reorients the LC director by the optical Kerr alignment, and this has been well documented since as early as 1973.[1−3] Adding a small amount of dye (1−2%) to the LCs reduces the threshold by 2 orders of magnitude due to interaction of the dye molecules with the surrounding LCs host.[4−7] More recently, our group has reported optical reorientation properties of planar nematic 4′-penthyl-4-cyanobiphenyl (5CB) thin film using a focused near-infrared laser beam with an intensity of 45 MW/cm^2.[8] In this earlier study, the tightly focused laser beam not only reorients local LC directors around the focal spot area but also induces optical trapping and manipulation of point or line (disclination) defects. The latter finding demonstrates a gradient force exerted by the focused beam on the defects in the homogeneous anisotropic LCs, and this phenomenon is further documented by Smalyukh et al.[9,10] For a two-component system, focused laser beams with low power intensity can be used as laser tweezers to trap microsized colloids in nematic LCs.[11−14] Laser trapping of the colloidal particles with refractive index being lower than those of the birefringent LC medium has been proposed to involve two mechanisms; below OFT threshold, the laser trapping of the colloidal particles is due to anisotropic dielectric interaction between the polarized light and the inhomogeneous distribution of director around the particle, and above OFT threshold, it is mediated by interaction between the optically distorted region of the elastic LCs and the particle.[11,13] In other cases, a focused laser beam has been demonstrated to trap spherical LC droplets in nonmiscible host fluid (generally water), where conventional laser trapping is addressed to their high refractive index and birefringence.[15−17] Interestingly, the radial symmetry organization inside the birefringent droplets is broken by the optical tweezers, leading to angular momentum transfer and laser-induced rotations of the droplets.[16−19]

The richness of their optical trapping phenomena makes LCs useful for laser-trapping measurements to decipher the interplay between molecular reorientation and a tightly focused laser beam, similarly to laser-trapping crystallization.[20,21] Such alignment control of the trapped molecules enabling crystal polymorph control by the laser beam has attracted great attention,[21,22] and it is one of key information, together with molecular diffusion and convection flow from surrounding area to the focal point,[23,24] to understand the laser-induced crystallization process. Moreover, optical Kerr alignment with induced-dipole interaction energy being in the order as small as 10^{-4} k_BT (where k_B is the Boltzmann constant and T is the Kelvin temperature) cannot be attributed to laser-induced crystallization process, which takes place on short time scales.[25−27] Instead, mutual cooperative motions due to dipolar interactions have been proposed to play a key role.[26,27] Therefore,

Received: January 24, 2011
Revised: May 18, 2011
Published: June 02, 2011

Scheme 1. (A) Schematic Diagram of the Experimental Setup,[a] (B) Schematic Diagram of the LC Cell Assembled from Glass Plates Coated with PVA Thin Layer, and (C) Chemical Structure of 5CB

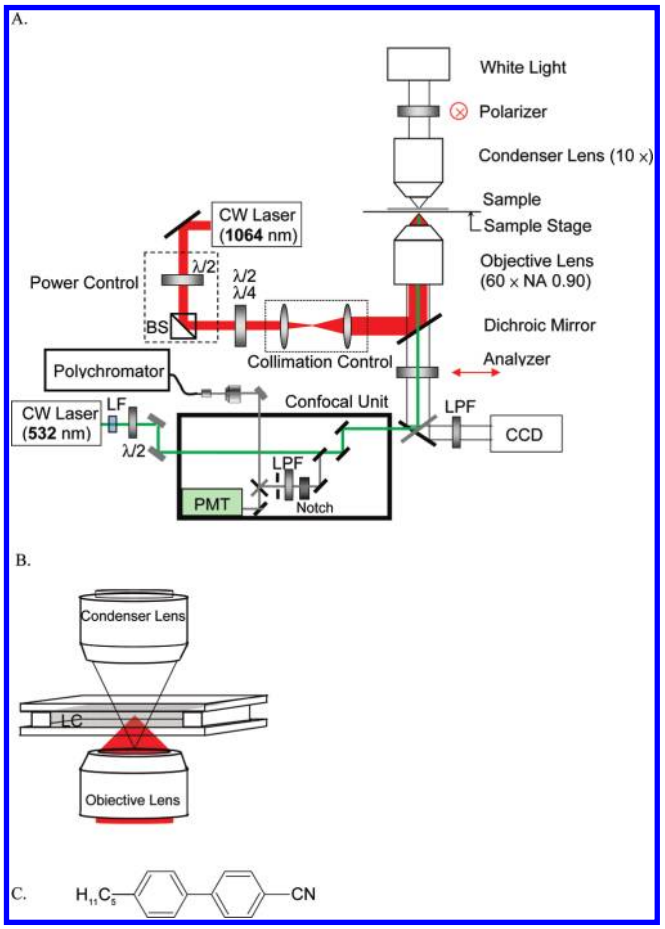

[a] BS = beam splitter, $\lambda/2$ = half-wave plate, $\lambda/4$ = quarter-wave plate, LF = line filter, and LPF = short pass filter with transmission edge at 900 nm.

such fundamental study of introducing a highly focused laser beam in a homogeneous LCs is of great significance and will provide new insights into reorientational motions in LCs.

We have previously reported that laser beam with intensity above the primary OFT threshold focused at normal incidence in a nematic 5CB thin slab (Scheme 1) can induce collective molecular reorientation locally around the focal spot area.[8] In this work, we report on experimental observations of optical reorientation of the LCs and its transformation to a new metastable domain induced by a tightly focused laser beam with higher power intensity. The domain nucleates at the focal spot and grows with irradiation time up to a dimension much larger than that of the focal spot. This experimental finding provides some information about local laser manipulation in planar nematic LC slab by a focused laser beam. We consider qualitatively that the domain is formed by optical reorientation of the LCs with refractive index mismatch compared with the surroundings, acting as a micrometer-sized "ghost particle" and generating gradient force exerted by the focused beam, and the gradient force is balanced by interfacial tension and elastic forces from the nematic surroundings. Further we have determined both the power density and polarization dependences of the domain formation and characterized the molecular alignment and density at the beam center using polarized Raman microspectroscopy and imaging.

2. MATERIALS AND METHODS

The LC cell was assembled from two cover-glass plates (Matsunami; 40 × 24 cm, thickness 120−170 μm), which were spin-coated with poly(vinyl alcohol) (PVA) thin layer and rubbed with lens tissue along one direction. The thickness of the cell chamber (~16 μm) was obtained by using strips of parafilms along glass edges, and the chamber was filled with 5CB (Tokyo Kasei Co.). The LC cell was put and fixed on sample stage between a pair of orthogonal polarizers on an inverted-microscope (Olympus IX71) system.

The experimental setup is schematically shown in Scheme 1. A continuous wave Nd:YVO_4 laser beam (λ = 1064 nm) (Spectra Physics; J20I-BL-106C) acting as a trapping beam was focused at normal incidence into the LC cell through an objective lens (UPlanApo; magnification = 60×, 1064 nm transmittance = 60%, and NA = 0.90). The beam waist (ω_0) and focal beam cross section were calculated to be 1.44 μm and 1.63 × 10^{-8} cm^2, respectively. Power of the 1064 nm laser beam was varied in the range 0.4−1.4 W after the objective lens, and its polarization state was controlled properly using half-wave or quarter-wave plate. The vertical position of the focal volume in the LC cell was controlled precisely (with a resolution of 0.1 μm) by adjusting the longitudinal position of the objective lens using a stepping motor, while the LC cell is fixed on the sample stage.

The optical reorientation of the LC director was analyzed conventionally by detecting the transmittance of visible probe light from a halogen lamp (λ = 400−750 nm) passing through the crossed polarizers by using a charge-coupled device (CCD) camera (JAI; CV-A55IR E) running at 30 interlaced frames/s. The elastic light scattering of the laser beam was cut by putting a short pass filter (with the transmission edge at 900 nm) before the CCD camera. The optical reorientation was also monitored by detecting Raman scattering light of excitation beam (532 nm, 40 mW) in the backward direction. The excitation beam was introduced into the LC cell through a confocal unit and the objective lens. The confocal Raman scattering signal from a confined focal volume as small as 4.65 μm^3 was passed through a notch filter for suppressing the Rayleigh scattering and then through a confocal pinhole onto a single grating by an optical fiber. The signal was then detected using a CCD-coupled polychromator (Princeton Instruments; SpectraPro 2300i). With 532 nm laser excitation, 600 lines/mm grating, and 1340 pixels, spectral resolution of Raman spectrum was in the range 2.4−3.4 cm^{-1}. The signal was also detected by a photomultiplier tube, and it was converted into Raman image by Olympus FV300 software. All experiments were carried out at room temperature (23−24 °C).

3. RESULTS

3.1. Polarized-Light Microscopy Image. In order to characterize the initial phase of the 5CB thin film in the LC cell, before introducing the 1064 nm laser beam, we have measured the transmittance of visible probe light at different angle between rubbing direction and analyzer by rotating the sample stage. The intensity of the transmitted light within the detection area of 100 × 70 μm has been well fitted with a sinusoidal function (data not shown), confirming that the 5CB slab adopts a homogeneous

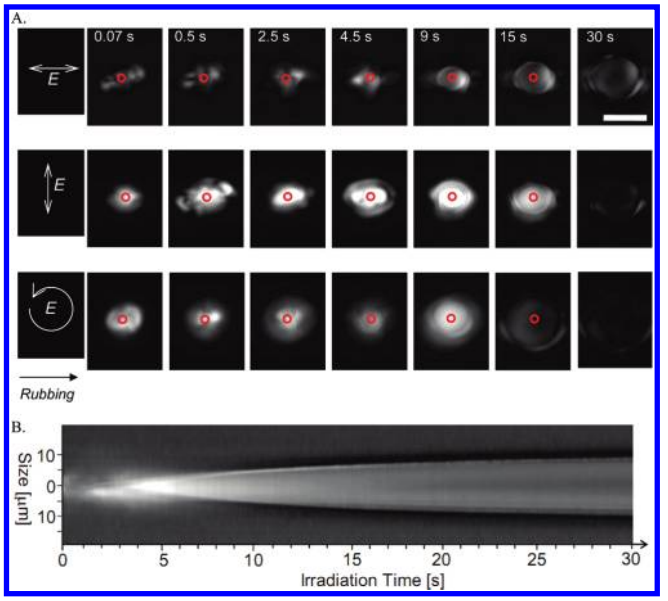

Figure 1. (A) Sequences of time evolution snapshots obtained by crossed polarization microscopy, showing dynamic optical reorientation of nematic 5CB thin film induced by a tightly focused laser beam with different polarization state as indicated in the left column of each sequence. Each column is taken at the same irradiation time. The power of the near-IR laser trapping beam was 1.2 W. The red circle in each image represents the focal spot, and it has been omitted in the snapshots at 30 s for the sake of clarity. The scale bar of 10 μm is applied for all images. (B) Spatiotemporal images showing the optical reorientation at the focal spot and its surroundings, followed by the formation a single spot at the center of the laser beam under continuous irradiation of linearly polarized laser beam with light electric field vector being parallel the rubbing direction.

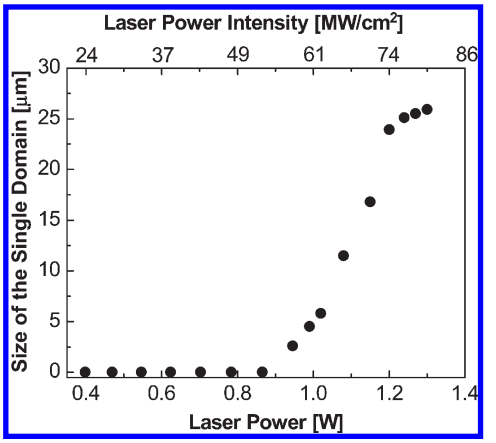

Figure 2. Plot dependence of the size of the single spot at long irradiation time (100 s) as a function of the laser power intensity for the case of linear polarized laser beam with light electric field being parallel to the rubbing direction.

nematic state with the director being parallel to the rubbing direction. The sample stage was then fixed with a configuration where the rubbing direction of the LC cell is parallel to the analyzer, allowing us to have a dark background before laser irradiation.

We found that a static single spot of transmittance around the focal area was observed at laser power intensity of 0.7 W (or 43 MW/cm^2) in accordance with our earlier report.[28] Upon focusing laser beam with high power intensity at 1.2 W (or 73.6 MW/cm^2), the LC thin film indeed shows unusual dynamics of spatiotemporal photoresponse as indicated by time evolution of transmittance in the cross-polarization microscopy images as shown in Figure 1A. For linearly polarized laser beam with the electric field being parallel to the rubbing direction (Figure 1A; first row), nonsymmetric shape of transmittance was observed in the area up to the distance of ~10 μm around the beam center (see snapshots at 0.07−2.5 s). The transmittance shows temporal dynamics in the shape and size, and it ultimately converts into a single spot at the beam center on a few seconds time scale (see snapshots at 4.5 s and longer times). The single spot grows continuously with the laser irradiation time as shown by the continuous spatiotemporal image depicted in Figure 1B, where it reaches the mean diameter of 24 μm at irradiation time of ~100 s. The single spot also shows spatiotemporal dynamics, where its transmittance at the focal point is the brightest at around 9 s, and it decays with the growth of the single spot. The appearance of the dark area around the beam center is clearly observed at irradiation times longer than 25 s, as shown in the snapshot at 30 s. When the laser beam is switched off, the single spot disappears immediately into the initial nematic phase with a characteristic relaxation time of ~70 ms. This relaxation time was obtained by fitting the decrease of the spot size with a single-exponential decay function, as the orientational free relaxation is governed by a simple exponential law.[5] Reproducibility of the formation and annihilation of the domain were observed repeatedly by switching on and off the laser beam, respectively.

To investigate the effect of polarization state, we then exposed the sample to the equal intensity of laser beams with linear polarization having a light electric vector being perpendicular to the rubbing direction or with circular polarization. We used the same LC cell to ensure the identical morphology of the sample before irradiation. The focal point is located at the same position in the LC cell; therefore, the focal position effect for the different polarization beams can be neglected. As shown in the sequences of time evolution snapshots in Figure 1A, the different polarization state readily induces different dynamics of transmitted probe light from the early irradiation time, indicating that polarization state is crucial to determine the degree of optical reorientations of LCs at the focal volume and its vicinity in the early irradiation time as well as in their further dynamics.

At the early irradiation time, the intensity of transmitted probe light is always higher when the LC thin film was irradiated by linearly polarized laser beam with light electric vector being perpendicular to the rubbing direction, as compared to those under the other polarization states. This indicates that the optical fields polarized perpendicular to the rubbing direction lead to an initial in-plane rotation of the nematic directors, resulting in greater transient transmission through crossed polarizers. Therefore, the degree of optical reorientation and birefringence effect are highly induced under such a configuration. In comparison, the circularly polarized beam gives weaker but wider area of transmittance. The latter is most probably due to the rotated light electric vector, which can induce nonlinear rotations leading to transverse nonlocal effects in the LC thin slab.[29,30] At irradiation times shorter than 15 s, domains of the transmittance with the polarization dependence of brightness, shape, and size are observed in all polarization states, and at longer irradiation times, ultimately the domains show almost similar brightness and shape.

3.2. Laser Power Dependence. By varying the laser power, we found that the formation of the dynamic transmittance is only observed when the laser power is above 0.9 W, corresponding to

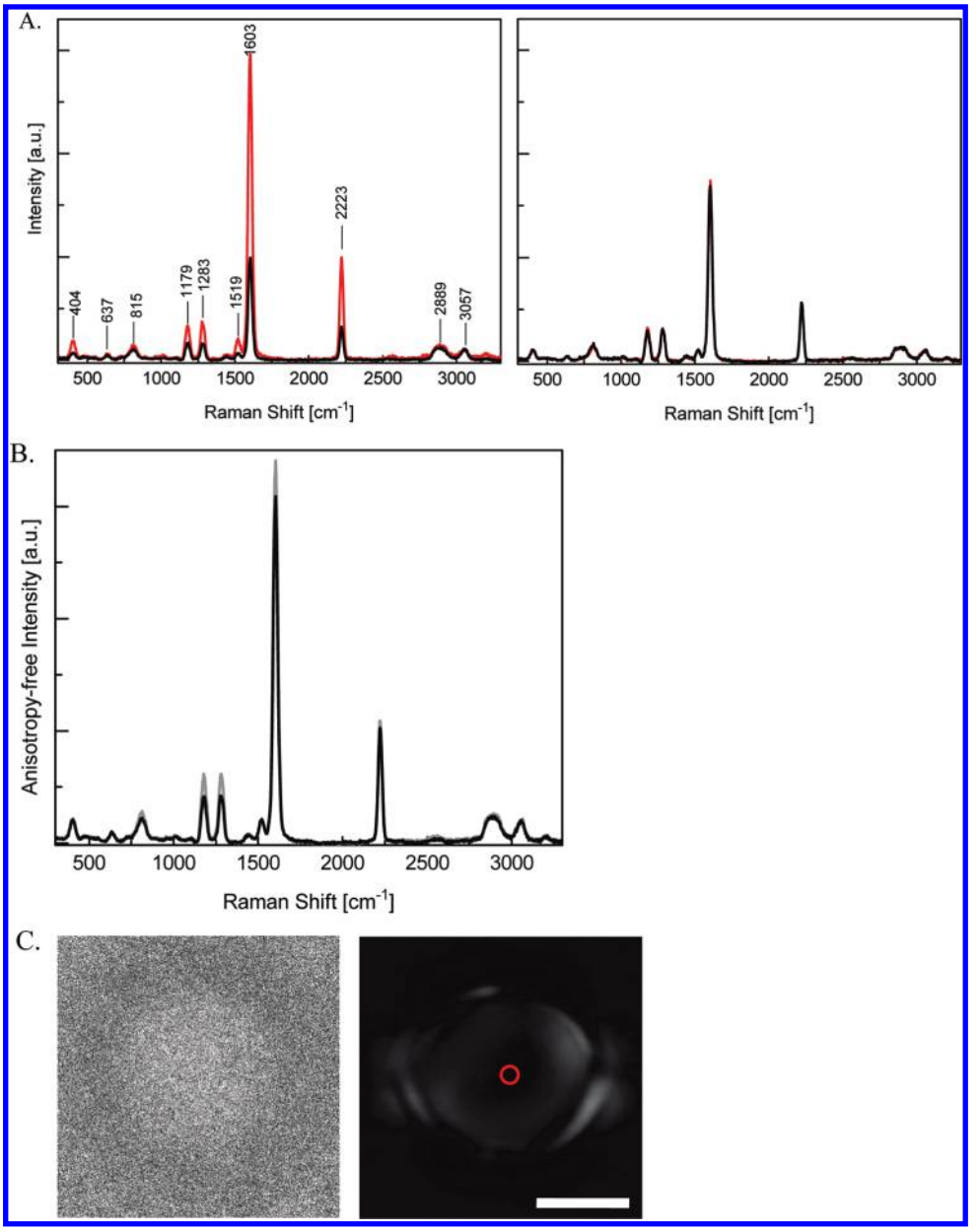

Figure 3. (A) Raman spectra for the polarization of the excitation beam parallel ($A_{parallel}$; red lines) and perpendicular ($A_{perpendicular}$; black lines) to the homogeneous anisotropic 5CB before irradiation (left panel) and after the formation of the metastable domain measured at 100 s after the laser irradiation (right panel). All spectra were accumulated for 2 s. (B) Anisotropy-free Raman spectrum calculated as $(2A_{perpendicular} + A_{parallel})/3$ before irradiation (black line) and after the formation of the metastable domain (gray line). (C) Raman image (left) of the formation of metastable domain measured at 100 s after the laser irradiation and the crossed polarization microscopy image (right) taken at the same time of laser irradiation. The Raman image was collected for 2.5 s. The red circle representing the focal spot size and the scale bar of 10 μm apply for both images.

laser power intensity of 56 MW/cm^2, as shown in Figure 2 for the light electric field parallel to the rubbing direction. The increase in the laser power intensity, above the threshold, results in nonlinear increase in the dimensions of the single spot, but when the laser power reaches the saturation level (~76 MW/cm^2), the single spot is no longer increased, suggesting a limit of the single spot dimension in the LC thin film with the particular thickness. Upon changing the polarization state, the threshold is almost the same and reproducible within 56−58 MW/cm^2 for all polarization states.

3.3. Raman Microspectroscopy. Raman spectra from the confined focal volume of the 5CB thin slab before irradiation and those after the formation of the single spot are depicted in Figure 3A. The spectra represent the peaks intensities within 300−3300 cm^{-1} as a function of the polarization of incident Raman excitation beam, i.e., $A_{parallel}$ and $A_{perpendicular}$ for excitation beam parallel and perpendicular, with respect to the rubbing direction. All the spectra show the major characteristic bands of 5CB with Raman shifts at 404, 637, 815, 1179, 1283, 1519, 1603, 2223, 2889, and 3057 cm^{-1}. In general, the frequency positions and relative intensity of the bands are consistent with those reported in the literature.[31−34] Those bands have also been assigned to out-of-plane and in-plane vibrational modes of the aromatic rings (637, 815, 1179, 1283, 1519, 1603 cm^{-1}), out-of-plane and stretching vibrations of CN cyano group (404 and 2223 cm^{-1}),

dx.doi.org/10.1021/jp200721f |J. Phys. Chem. C 2011, 115, 11906–11913

and stretching CH vibrations of the alkyl group (2889 cm^{-1}) and the aromatic rings (3057 cm^{-1}).[32] The dichroic ratio ($A_{parallel}/A_{perpendicular}$) of the in-plane vibrational bands of the aromatic and CN cyano group in the fingerprint region before irradiation is ~3, indicating that they have a strong dichroism and in good agreement with the published data.[31,35] We note that without the 1064 nm laser irradiation the $A_{parallel}$, $A_{perpendicular}$, and the dichroic ratio are constant, ensuring that the Raman excitation beam does not induce optical reorientation in the 5CB slab.

One can find that such a strong dichroism disappears and the dichroic ratio becomes ~1 at the focal volume at the extended irradiation times. Importantly, the anisotropy-free spectrum at the focal volume shows an intensity increase and spectral reshaping as compared to that before irradiation, but no frequency shift is observed, as depicted in Figure 3B. The increase is observed particularly for the in-plane vibrational bands of aromatic and CN cyano group in the fingerprint region. We should stress that such a total Raman intensity is enhanced only under the focused laser beams with high power intensity, or otherwise it remains substantially unchanged at low intensity laser beams. As shown in Figure 3C, shape and size of the domain observed by using Raman imaging agree with those observed by using crossed-polarization microscopy. The anisotropy-free Raman image clearly shows an intensity distribution around the domain, displaying higher intensity inside the domain, in contrast to lower intensity near the edge extending to the outer area.

4. DISCUSSION

4.1. Optical Reorientation at Early Laser Irradiation. The transmittance of probe light in the cross-polarization microscopy images can be attributed to laser-induced local director modulation or optical reorientation in the anisotropic 5CB thin slab as a response of 5CB to be parallel to the light electric field due to its positive optical dielectric anisotropy.[2,36,37] The intensity of transmittance is related explicitly to local optical reorientation and photorefraction efficiency of the 5CB thin film.[38] The optically induced reorientation of a nematic LC slab by a focused laser beam has been investigated theoretically and experimentally by Khoo et al.,[39] where by taking into account the balance between the generated optical and preexisting elastic torques (bend, splay, and twist) of the LCs, they have demonstrated that reorientation transverse profile is dependent on the ratio between the beam waist (ω_0) relative to the thickness of the slab (d) and light electric field.[39] Using the relation between the width of reorientation and ω_0/d,[39] we estimated that for $\omega_0 = 1.44\ \mu m$ and $d = 16\ \mu m$ the width of reorientation to be about 3.7 μm. This value is comparable to our single spot size (3.8 μm) of transmittance for the static reorientation at laser power intensity of 43 MW/cm^2. Thus, the nonsymmetric shape of transmittance at the early irradiation time, as shown in Figure 1A, can be considered as the transverse profile at the higher laser power intensity. The large variations of the transverse profile are due to the different polarization state, which determines the degree of optical reorientation.

4.2. Domain Formation at Long Irradiation Time. At first glance, the sequences of crossed polarization microscopy images indicate the spatiotemporal dynamics of optical reorientation induced by the focused laser beam in the anisotropic 5CB thin slab. From the optical viewpoint, such orientational deformations can be considered as nonsingular defects in a uniaxial 5CB monocrystal. In the other words, a spatially inhomogeneous refractive index pattern is induced in the anisotropic alignment from the early irradiation time. The local effective refractive index within the optically destabilized area can jump from ordinary to extraordinary refractive index, or it can be varied within some fraction of optical anisotropy depending on both the polarization state and the actual local director.[40] Considering that the effective refractive index in the elastic deformation of anisotropic LC might be modulated up to the scale of micrometers, the abrupt change of LC directors is not preferred in terms of the elastic free energy.[41] Such local optically reoriented LCs with refractive index mismatch compared to that of surroundings should also be regarded as laser-induced defects, although they are readily different from point defects or disclinations which exist in many nematic structures due to misalignment. Therefore, we may consider that they can act as a microsized "ghost particle", similarly to that particular particle proposed by Muševič et al.[11] for the optically induced distortion or local decrease of the order parameter of a birefringent nematic LCs containing colloids.

The highly focused laser beam then can induce axial trapping or generate repulsive force on the ghost particle at the focal point with both the magnitude of optical gradient force and interaction energy being determined by the changes in the local refractive index and the laser power intensity.[9,42] For an axially symmetric Gaussian laser beam, the particle can be trapped at the focal point in a similar way to high-refractive index nano- to microsized colloidal particles when their index are higher compared to surroundings and when the necessary energy condition for optical trapping is satisfied,[14,43−45] or it may also be trapped unconventionally as a consequence of either the interaction between the ghost particle and distorted surroundings in the elastic medium[11,13] or faster shape alteration of the particle than its expulsion out of the focal point due to its deformability.[46] Attractive or repulsive force on the ghost particle should be accompanied by further reorientation in the surrounding area through elastic dipolar interactions to minimize the free energy of the system. Therefore, under continuous intense laser irradiation, the optical reorientation, the generated attractive or repulsive force, and elastic torques due to intermolecular dipolar interactions lead the LCs to complicated reorientation dynamics at the focal point and its vicinity. We note that the dynamic reorientations must induce fluctuations in spatial distribution, intermolecular spaces, and dipolar attractive interactions. This issue, in principle, has been shown in recent work on singular birefringent patterns in homogeneous LCs induced by light beams.[47]

The dynamic orientational transitions induced by linearly polarized light at normal incidence to the layer of nematic LCs have been studied theoretically based on the balance of torques acting on the director, where above a bifurcation the unsteady dynamics settles to a new stationary distorted state.[48] Since the experimental geometry is similar to our experiment, we may consider qualitatively that the optical reorientation and generated trapping or repulsive force on the ghost particle in the focal volume, in principle, is equalized by elastic forces, viscosity, and interfacial tension from the surroundings as well as the anchoring effect of the rubbed polymer surface, resulting ultimately in a new equilibrium state. The similar brightness and shape of domains at long irradiation times under different polarization state may also suggest that the LCs organization in the domains is not determined solely by the polarization direction, but it is rather determined by the interplay between those forces in the equilibrium state, minimizing the elastic free energy inside the

domains and its surroundings. Such an equilibrium state can also be therefore considered as a local minimum with a total free energy lower than that of the optical reorientation but higher than the nematic alignment. Thus, the equilibrium state, which nucleates at the focal volume, tends to grow through cooperative motions, leading to its volume polarizability enhancement and greater optical gradient force[49] and allowing this state to propagate out of the focal volume with the irradiation time.

The disappearance of the domain upon switching off the laser beam can be attributed to the restoring the initial nematic alignment by anchoring effect of the polymer surface coated on the substrates and by bulk elastic torques of the nematic environment. Reproducibility of the formation and annihilation of the metastable domain upon switching on and off the laser beam implies the absence of memory after the irradiation. It is worth mentioning that this feature is similar to the laser-induced manipulation of a disclination line and texture in LCs,[8,9] but it is in contrast to the destabilization of nematic structure of LC thin films containing photochromic compounds, which require photoinduced back-isomerization to achieve the recovery of the initial anisotropic phase.[50,51]

4.3. Possible Microscopic Densification. Since the in-plane vibrational modes of the aromatic and CN cyano group in the fingerprint region are oriented predominantly parallel to the molecular dipole, and since the intensity of Raman band is proportional to the square of the induced dipole, polarized Raman bands of 5CB have been used to characterize molecular alignment of the LC thin film.[31,34] Using similar alignment analysis, the strong dichroism of the Raman bands before irradiation (Figure 3A) suggests that the local LC director is parallel to the rubbing direction, supporting the result of polarization microscopy (see section 4.1). The changes in the dichroic ratio indicate the optical reorientation, and when the ratio is equal to 1 (at long irradiation times), it suggests plausibly that depolarization ultimately takes place at the beam center.

In Figure 3B, the anisotropy-free Raman spectrum is shown to have a spectral reshaping and an intensity increase when the domain is formed. The spectral reshaping is most probably due to modifications of dipole distribution, particularly those of the out-of-plane bending (400−900 cm^{-1}) and in-plane stretching vibrations (2800−3300 cm^{-1}) of CH bonds of the alkyl and aromatic groups, as they are sensitive to intermolecular forces and internal rotations.[34] Since sufficiently high temperature accompanying phase transition can induce spectral shifts in 5CB[32,34] or high pressure can induce similar effect in other aromatic compounds,[52] the absence of spectral shifts caused by the laser beam at the focal point suggests that the effects of local temperature and pressure elevation can be neglected.

To estimate the local temperature elevation, we have taken the linear relation between local temperature increase (ΔT) at the beam center and the incident near IR laser power (P), as given by $\Delta T/P = A_{abs}/2\sqrt{\pi\kappa r_0}$,[53,54] where $A_{abs} = \alpha z_0/2.3$ is the total absorption of 5CB at 1064 nm, α is the extinction coefficient, z_0 is the axial size of the focal volume ($z_0 = 1.4 \times \lambda \times n/(NA)^2 = 2.85$ μm for the average refractive index of 5CB, $n = 1.55$), κ is isotropic thermal conductivity, and r_0 is the beam radius ($r_0 = 0.5w_0 = 0.61 \times \lambda/NA = 0.72$ μm). From the reported values of $\alpha \approx 0.01$ cm^{-1} [8,55] and $\kappa = 1.96 \times 10^{-3}$ W cm^{-1} $°C^{-1}$,[56] we estimated the temperature elevation at the focal spot to be 2.5 °C/W. This means that it is 3 °C by the focused laser beam with the power of 1.2 W. On the other hand, the magnitude of photon pressure exerted on the 5CB is typically within a few hundreds of pN depending on the refractive index mismatch.[12,14] Thus, the photon pressure at the waist of the trapping beam is calculated to be within the order of kPa, which is much lower than that to induce frequency shifts of Raman bands.[57]

Importantly, since average molecular polarizability of 5CB in different phases from nematic to isotropic is almost unchanged,[58] and since the nonresonant 1064 nm laser irradiation does not induce any molecular conformational changes in 5CB, the anisotropy-free or total micro-Raman intensity can be therefore related to the local density in the confined focal volume.[59] Thus, we proposed that the enhancement of the total Raman intensity is attributable to densification. Such a possible densification most probably provokes (i) the internal rotations of the aromatic rings and alkyl group, rather than conformational changes such as in the photoinduced contractions of LC elastomers containing photochromic azobenzene,[60] and (ii) spatial LCs deorientation or displacement within the domain and its outer area. However, one may consider that there must be modifications of the optical path and transmittance of the Raman excitation beam due to the changes in molecular orientation and local birefringence upon the domain formation, leading to enhancement of the Raman scattering efficiency. These lens effects will be examined and made clear in the future work by measuring the total Raman intensity as a function of the distance from the focal point.

4.4. Laser Power Dependence of the Domain Formation. It has been established that the laser trapping properties can be controlled by several ways, such as changing the beam polarization, varying the laser power, etc.[21,22] For the anisotropic LCs, we found that although the polarization state determines the degree of optical reorientations, the new metastable domain is formed almost at the same time under the same power of continuous laser irradiation. This strongly suggests that the optical trapping is generated by all those polarization states, and gradient force is generated depending on the optical field intensity (see Figure 2). Since the OFT threshold of the nematic 5CB thin slab with a thickness of 16 μm would be in the order of a few hundreds kW/cm^2, considering the OFT threshold of 0.16 and 2.2 kW/cm^2 for 250 and 65 μm, respectively, reported in early studies,[2,3] the definite optical intensity threshold to generate the domain is more than 2 orders of magnitude larger than the OFT threshold for all the polarization states. This also indicates that the domain is generated by the high optical field involving the optical reorientation and gradient force, which leads to optical trapping and reorganization of the LCs as described in section 4.2, rather than simply the optical Kerr reorientation. Thus, one possible qualitative explanation for high threshold power for the domain formation could be the minimum free energy of the attractive force to overcome interfacial tension and bulk elastic force exerting on the domain formation, similarly to that demonstrated in laser-induced phase separation.[61] We also consider that in the anisotropic LCs the reorientation energy should be polarization dependent, and thus, the equilibrium condition, in which the attractive force is balanced by interfacial tension, viscosity, and bulk elastic force, should depend on the polarization state of laser beam. However, in this case, though early dynamics in fact is polarization dependent (Figure 1A), the equilibrium condition is accidentally independent of the polarization state, as indicated by the comparable optical intensity threshold under laser irradiation with different polarization states. This may further indicate that the equilibrium condition is achieved through cooperative motions and reorganization of the LCs in vicinity of the focal volume, which are not directly optically reoriented. Another possible explanation is that if the longitudinal field is most

important in governing reorientation outside the focal volume, particularly the longitudinal field should be small for the highly focused beams under the polarization conditions employed; the threshold for the domain formation therefore appears artificially at high power intensities.

4.5. Depolarized Alignment at the Beam Center. While the metastable domain grows with the irradiation time, its clear interface suggests that molecular alignment inside it is distinct from the surrounding phase. The dark area around the domain center can be attributed either to restoring the nematic alignment, to orientation → deorientation, or to a microscopic nematic → isotropic transition. Considering that the dichroic ratio is equal to 1 after long irradiation times, restoring the nematic alignment at the focal point is highly unlikely to occur, but in contrary, the dichroic ratio strongly indicates depolarization leading to deorientation or a nematic → isotropic transition, particularly around the beam center. Since the trapping beam induces the temperature elevation at the beam center as high as 3 °C from the room temperature (23−24 °C), as mentioned in section 4.3, this finding reveals the possibility of local nematic → isotropic transition for 5CB around the beam center that occurs below the normal phase-transition temperature (34−35 °C).[32,62] We consider that this is due to either the complicated geometry of the condensed beam at the focal point,[63] reshaping wavefront profile of the laser beam because of the spatially nonuniform refractive index patterns after the first optical reorientation or the elastic torques from the surroundings in the equilibrium state. This finding clearly shows the qualitative difference in the behavior to that of solute−solvent systems, where phase transition or phase separation in the two-component systems, such as aqueous solution of glycine, triethylamine, or sodium dodecyl sulfate/xylene/1-pentanol, is thermodynamically and directly driven by radiation pressure of the laser trapping beam without any effects of the solvent.[23,28,61,64]

From the nonzero transmittance in the surrounding area of the beam center in the polarization microscopy images of the domain (Figure 1A), we can draw a conclusion that the order parameter of local 5CB directors out of the center area are not zero, or in other words, they are locally nematic alignments with various order parameters. Since such a polarization microscopy also does not show an image of a typical radially symmetric LC droplet,[17,65,66] one of the possible configurations inside the domain is a rotational symmetry with respect to the beam center, though the detail molecular configuration is still an open question and might be a subject of future study.

5. CONCLUSIONS

We have presented a study of optical reorientation of homogeneous nematic 5CB thin slab induced by a highly focused near-infrared laser beam. The optical reorientation behavior shows unusual behavior when laser power intensity is higher than 56 MW/cm^2, as the optically reoriented LCs shows the spatiotemporal dynamics and ultimately transforms to a new metastable domain, which nucleates at the focal spot and grows with the irradiation time up to the diameter of a few tens times larger than the focal size. We consider that the optically reoriented LCs with refractive index mismatch compared with the surroundings can act as a microsized "ghost particle", and for this reason an optical gradient is generated and exerted on the particle in the focal point, leading to its optical trapping and manipulation. Laser trapping process is supported by the unique intensity increase in the anisotropy-free Raman spectrum and imaging at the confined focal volume. This finding may be an indicative of a possible microscopic densification by the tightly focused laser beam. The change in dichroic ratio at the beam center from 3 to 1 at long irradiation time can be attributed to depolarization leading to local orientation → deorientation or isothermal microscopic nematic → isotropic phase transition. The nucleation and growing of the micrometer-sized metastable domain is a unique merit of the optical reorientation of 5CB thin slab induced by a highly focused laser beam, providing experimental evidence of optical control of a great number of molecules in a single-component system by the focused laser beam.

AUTHOR INFORMATION

Corresponding Author

*E-mail: usman@faculty.nctu.edu.tw (A.U.), uwada@mail.nctu.edu.tw (T.U.), masuhara@masuhara.jp (H.M.).

ACKNOWLEDGMENT

The present work has been supported by the MOE-ATU Project (National Chiao Tung University) from the Ministry of Education of Taiwan, the National Science Council of Taiwan to T.U. (NSC 98-2113-M-009-013-MY2) and to H.M. (NSC 98-211-M-009-001), a KAKENHI grant (a Grant-in-Aid for Scientific Research) in the Priority Area "Molecular Science for Supra Functional Systems" to T.U., and a KAKENHI (S) grant (18106002) to H.M. from the Japan Society for the Promotion of Science (JSPS).

REFERENCES

(1) Wong, G. K. L.; Shen, Y. R. *Phys. Rev. Lett.* **1973**, *30*, 895.
(2) Durbin, S. D.; Arakelian, S. M.; Shen, Y. R. *Phys. Rev. Lett.* **1981**, *47*, 1411.
(3) Santamato, E.; Daino, B.; Romagnoli, M.; Settembre, M.; Shen, Y. R. *Phys. Rev. Lett.* **1986**, *57*, 2423.
(4) Jánossy, I. *Phys. Rev. E* **1994**, *49*, 2957.
(5) Simoni, F. *Nonlinear Optical Properties of Liquid Crystals and Polymer Dispersed Liquid Crystals*; World Scientific Publication Co.: London, 1997.
(6) Jánossy, I. *J. Nonlinear Opt. Phys. Mater.* **1999**, *8*, 361.
(7) Fuh, A. Y.-G.; Liao, C.-C.; Hsu, K.-C.; Lu, C.-L. *Opt. Lett.* **2003**, *28*, 1179.
(8) Hotta, J.; Sasaki, K.; Masuhara, H. *Appl. Phys. Lett.* **1997**, *71*, 2085.
(9) Smalyukh, I. I.; Kaputa, D. S.; Kachynski, A. V.; Kuzmin, A. N.; Prasad, P. N. *Opt. Express* **2007**, *15*, 4359.
(10) Smalyukh, I. I.; Senyuk, B. I.; Shiyanovskii, S. V.; Lavrentovich, O. D.; Kuzmin, A. N.; Kachynski, A. V.; Prasad, P. N. *Mol. Cryst. Liq. Cryst.* **2006**, *450*, 279.
(11) Muševič, I.; Škarabot, M.; Babič, D.; Osterman, N.; Poberaj, I.; Nazarenko, V.; Nych, A. *Phys. Rev. Lett.* **2004**, *93*, 187801.
(12) Smalyukh, I. I.; Kuzmin, A. N.; Kachynski, A. V.; Prasad, P. N.; Lavrentovich, O. D. *Appl. Phys. Lett.* **2005**, *86*, 021913.
(13) Škarabot, M.; Ravnik, M.; Babič, D.; Osterman, N.; Poberaj, I.; Žumer, S.; Muševič, I.; Nych, A.; Ognysta, U.; Nazarenko, V. *Phys. Rev. E* **2006**, *73*, 021705.
(14) Smalyukh, I. I.; Kachynski, A. V.; Kuzmin, A. N.; Prasad, P. N. *Proc. Natl. Acad. Sci. U.S.A.* **2006**, *103*, 18048.
(15) Joudkazis, S.; Matsuo, S.; Murazawa, N.; Hasegawa, I.; Misawa, H. *Appl. Phys. Lett.* **2003**, *82*, 4657.
(16) Brasselet, E.; Murazawa, N.; Joudkazis, S.; Misawa, H. *Phys. Rev. E* **2008**, *77*, 041704.

(17) Brasselet, E.; Joudkazis, S. *J. Nonlinear Opt. Phys. Mater.* **2009**, *18*, 167.
(18) Murazawa, N.; Joudkazis, S.; Misawa, H. *Eur. Phys. J. E* **2006**, *20*, 435.
(19) Yang, Y.; Brimicombe, P. D.; Roberts, N. W.; Dickinson, M. R.; Osipov, M.; Gleeson, H. F. *Opt. Express* **2008**, *16*, 6877.
(20) Sugiyama, T.; Adachi, T.; Masuhara, H. *Chem. Lett.* **2007**, *36*, 1480.
(21) Rungsimanon, T.; Yuyama, K.; Sugiyama, T.; Masuhara, H.; Tohnai, N.; Miyata, M. *J. Phys. Chem. Lett.* **2010**, *1*, 599.
(22) Rungsimanon, T.; Yuyama, K.; Sugiyama, T.; Masuhara, H. *Cryst. Growth Des.* **2010**, *10*, 4686.
(23) Yuyama, K.; Sugiyama, T.; Masuhara, H. *J. Phys. Chem. Lett.* **2010**, *1*, 1321.
(24) Uwada, T.; Sugiyama, T.; Miura, A.; Masuhara, H. *Proc. SPIE* **2010**, *7762*, 77620N.
(25) Zaccaro, J.; Matic, J.; Myerson, A. S.; Garetz, B. A. *Cryst. Growth Des.* **2001**, *1*, 5.
(26) Matic, J.; Sun, X.; Garetz, B. A.; Myerson, A. S. *Cryst. Growth Des.* **2005**, *5*, 1565.
(27) Oxtoby, D. W. *Nature* **2002**, *420*, 277.
(28) Hotta, J.; Sasaki, K.; Masuhara, H. *J. Am. Chem. Soc.* **1996**, *118*, 11968.
(29) Brasselet, E.; Dubé, L. J. *Mol. Cryst. Liq. Cryst.* **2006**, *453*, 93.
(30) Brasselet, E.; Dubé, L. J. *Phys. Rev. E* **2006**, *73*, 021704.
(31) Camorani, P.; Fontana, M. P. *Mol. Cryst. Liq. Cryst.* **2007**, *465*, 143.
(32) Kang, D. S.; Kwon, K.-S.; Kim, S. I.; Gong, M.-S.; Seo, S. S. A.; Noh, T. W.; Joo, S.-W. *Appl. Spectrosc.* **2005**, *59*, 1136.
(33) Kachynski, A. V.; Kuzmin, A. N.; Prasad, P. N.; Smalyukh, I. I. *Opt. Express* **2008**, *16*, 10617.
(34) Babkov, L. M.; Gnatyuk, I. I.; Puchkovskaya, G. A.; Trukhachev, S. V. *J. Struct. Chem.* **2006**, *47*, 136.
(35) Nakano, T.; Yokoyama, T.; Toriumi, H. *Appl. Spectrosc.* **1993**, *47*, 1354.
(36) Ong, H. L. *Phys. Rev. A* **1983**, *28*, 2393.
(37) Khoo, I. C.; Michael, R. R.; Yan, P. Y. *IEEE J. Quantum Electron.* **1987**, *23*, 267.
(38) Khoo, I. C. *IEEE J. Quantum Electron.* **1996**, *32*, 525.
(39) Khoo, I. C.; Liu, T. H.; Yan, P. Y. *J. Opt. Soc. Am. B* **1987**, *4*, 115.
(40) Dunmur, D. A. Refractive Indices of Nematics. In *Physical Properties of Liquid Crystals: Nematics*; Dunmur, D. A., Fukuda, A., Luckhurst, G., Eds.; Inspec/IEEE Publication: London, 2001; pp 315−322.
(41) de Gennes, P. G.; Prost, J. *The Physics of Liquid Crystals*, 2nd ed.; Clarendon Press: Oxford, 1993.
(42) Tlusty, T.; Meller, A.; Bar-Ziv, R. *Phys. Rev. Lett.* **1998**, *81*, 1738.
(43) Neuman, K. C.; Block, S. M. *Rev. Sci. Instrum.* **2004**, *75*, 2787.
(44) Tsuboi, Y.; Shoji, T.; Kitamura, N. *J. Phys. Chem. C* **2010**, *114*, 5589.
(45) Ashkin, A.; Dziedzic, J. M.; Bjorkholm, J. E.; Chu, S. *Opt. Lett.* **1986**, *11*, 288.
(46) Murazawa, N.; Joudkazis, S.; Misawa, H.; Wakatsuki, H. *Opt. Express* **2007**, *15*, 13310.
(47) Brasselet, E. *Opt. Lett.* **2009**, *34*, 3229.
(48) Krimer, D. O. *Phys. Rev. E* **2009**, *79*, 030702.
(49) Louchev, O. A.; Joudkazis, S.; Murazawa, N.; Wada, S.; Misawa, H. *Opt. Express* **2008**, *16*, 5673.
(50) Ikeda, T. *J. Mater. Chem.* **2003**, *13*, 2037.
(51) Yu, Y.; Ikeda, T. *J. Photochem. Photobiol., C* **2004**, *5*, 247.
(52) Sun, B.; Dreger, Z. A.; Gupta, Y. M. *J. Phys. Chem. A* **2008**, *112*, 10546.
(53) Ito, S.; Sugiyama, T.; Toitani, N.; Katayama, G.; Miyasaka, H. *J. Phys. Chem. B* **2007**, *111*, 2365.
(54) Walgraef, D.; Ghoniem, N. M.; Lauzeral, J. *Phys. Rev. B* **1997**, *56*, 15361.
(55) Wu, S.-T. *J. Appl. Phys.* **1998**, *84*, 4462.
(56) Ahlers, G.; Cannell, D. S.; Berge, L. I.; Sakurai, S. *Phys. Rev. E* **1994**, *49*, 545.
(57) Zhao, L.; Baer, B. J.; Chronister, E. L. *J. Phys. Chem. A* **1999**, *103*, 1728.
(58) Li, J.; Wu, S.-T. *J. Appl. Phys.* **2004**, *96*, 6253.
(59) Favors, R. N.; Jiang, Y.; Loethen, Y. L.; Ben-Amotz, D. *Rev. Sci. Instrum.* **2005**, *76*, 033108.
(60) Finkelmann, H.; Nishikawa, E.; Pereira, G. G.; Warner, M. *Phys. Rev. Lett.* **2001**, *87*, 015501.
(61) Mukai, S.; Magome, N.; Kitahata, H.; Yoshikawa, K. *Appl. Phys. Lett.* **2003**, *83*, 2557.
(62) Faetti, S.; Palleschi, V. *Phys. Rev. A* **1984**, *30*, 3241.
(63) Koshioka, M.; Sasaki, K.; Masuhara, H. *Appl. Spectrosc.* **1995**, *49*, 224.
(64) Vekilov, P. G. *Cryst. Growth Des.* **2004**, *4*, 671.
(65) Brasselet, E.; Murazawa, N.; Misawa, H.; Joudkazis, S. *Phys. Rev. Lett.* **2009**, *103*, 103903.
(66) Xie, A.; Higgins, D. A. *Appl. Phys. Lett.* **2004**, *84*, 4014.